Pramana – J. Phys., Vol. 39, No. 4, October 1992, pp. 329–341. © Printed in India.

The effect of low intra-sublattice repulsion on phase diagram of $YBa_2Cu_3O_{6+x}$: A Monte Carlo simulation study

RITA KHANNA, T R WELBERRY and G ANANTHAKRISHNA*

Research School of Chemistry, The Australian National University, P.O. Box 4, Canberra, ACT 2601, Australia

*Materials Research Centre, Indian Institute of Science, Bangalore 560012, India

MS received 10 April 1992; revised 22 May 1992

Abstract. We report the results of Monte Carlo simulation of the phase diagram and oxygen ordering in $YBa_2Cu_3O_{6+x}$ for low intra-sublattice repulsion. At low temperatures, apart from tetragonal (T), orthorhombic (OI) and 'double cell' ortho II phases, there is evidence for two additional orthorhombic phases labelled here as $\overline{O}$I and OIII. At high temperatures, there was no evidence for the decomposition of the OI phase into the T and OI phases. We find qualitative agreement with experimental observations and cluster-variation method results.

Keywords. Oxygen ordering; phase diagram; $YBa_2Cu_3O_{6+x}$.

PACS No. 64·70

1. Introduction

It is now generally recognized that the oxygen stoichiometry in oxide superconductors is one of the most crucial parameters for their characterization and that the superconducting properties are very sensitive to the arrangement of oxygen atoms in the Cu–O basal plane. Various structural transitions in $YBa_2Cu_3O_{6+x}$ have been intensively investigated both from theoretical and experimental points of view (Zanbergen *et al* 1987; Cava *et al* 1987; Jorgenson *et al* 1987; Beyers and Shaw 1989; Beech *et al* 1987). One of the basic features of oxygen ordering is the tendency of oxygen to form O–Cu–O chains (Ceder *et al* 1990). There is enough experimental evidence for the existence of a tetragonal phase (T), the orthorhombic phase (OI) and a double cell orthorhombic phase (OII) (van Tendaloo *et al* 1987; Chen *et al* 1988; Specht *et al* 1988; Beyers *et al* 1989). However, the interpretation of other available data on structural phases and transitions in $YBa_2Cu_3O_{6+x}$ still remains somewhat ambiguous. There are reports of various additional orthorhombic superstructures, referred to as 'Magneli phases', in the region $x > 0{\cdot}5$ (Reyes-Gosga *et al* 1989). In addition, the occurrence of two phase regions (T and OI) at intermediate temperatures (Sood *et al* 1988) and the problems relating to T and OII phase boundaries at $x < 0{\cdot}5$ have not been fully understood. To some extent, theoretical studies have been hampered by the difficulty of distinguishing experimentally between stable and transient structures. A clear understanding of the phase diagram and various structural features associated with oxygen ordering in $YBa_2Cu_3O_{6+x}$ therefore assumes great importance.

Theoretically, apart from the work of Khachaturyan and Morris (1987, 1988), most treatments reduce the problem to a purely two dimensional ordering of occupied and vacant oxygen sites in the basal plane. The ordering can be described by means of a two-dimensional Ising model, proposed by de Fontaine *et al* (1987), with isotropic nearest-(J_1) and anisotropic next-nearest neighbour pair interactions (J_2 and J_3) between oxygen sites in the basal plane (see equation 1). That J_2 differs from J_3 reflects the effect of the mediating Cu ion in the latter case. Apart from some recent work using ab-initio calculations, most investigators have used: $J_1 = 1$, $J_2 = -0{\cdot}5$ and $J_3 = 0{\cdot}5$, as originally used by Wille and de Fontaine (1988). This choice of parameters has been traditionally used despite the fact that J_3 is only weakly repulsive. The interactions J_1 and J_2 being of chemical origin must be appreciably stronger than the purely Coulombic interchain repulsion J_3 (Mansurova *et al* 1990). In addition a proper choice of the sign and magnitude of J_3 is crucial to the stability of the ortho II phase. A positive J_3 will result in the complete disappearance of the ortho II phase. The object of the present work is to investigate the effect of lowering the strength of intrasublattice repulsion parameter J_3 on the phase diagram of $YBa_2Cu_3O_{6+x}$ in search of better interaction parameters. A proper choice of interaction parameters should be able to account for the various observed structural phases in $YBa_2Cu_3O_{6+x}$.

In a recent work using Monte Carlo simulations (Khanna *et al* 1992), we investigated the low temperature region of the oxygen deficient ($x < 0{\cdot}5$) region of the phase diagram with a reduced J_3 parameter ($J_3 = 0{\cdot}5$ to $0{\cdot}3$). The simulations were carried out at zero and high temperatures. The zero temperature simulation results had an interesting feature. For $J_3 = 0{\cdot}5$, there was clear evidence for three stable states, i.e., T, O II and O I. This result agrees well with other predictions of ground states for this set of interaction parameters (Stolze 1990). With decreasing magnitude of J_3, the ortho II region became narrower and narrower, finally disappearing completely at $J_3 = 0{\cdot}2$. This result is hardly surprising as the stability of the ortho II phase is governed by the strength of J_3 relative to that of J_2. Only the T and O I phases are stable with an attractive J_3 (Khachaturyan and Morris 1987). According to our simulation results, it now appears that the O II phase is not a stable ground state even for slightly positive values of J_3. With a view that a slightly positive J_3 might lead to the existence of Magneli phases and co-existing T and O I phases along with an O II phase, we have carried out Monte Carlo simulation of the phase diagram of $YBa_2Cu_3O_{6+x}$ using the following set of parameters: $J_1 = 1{\cdot}0$, $J_2 = -0{\cdot}5$ and $J_3 = 0{\cdot}2$. We examine the implications of our findings on the development of an adequate theoretical model.

2. Basic hamiltonian and Monte Carlo simulations

We use a lattice gas (2D Ising) model as was proposed by de Fontaine *et al* (1987), assuming anisotropic next-nearest neighbour interactions between oxygen sites. Figure 1 shows the basic lattice consisting of two interpenetrating square lattices and the effective pair interactions. An occupied site may be represented by spin $S_i = +1$ (up), an empty site by $S_i = -1$ (down). The Hamiltonian is equivalent to an Ising model in a magnetic field with three effective pair interactions J_1, J_2 and J_3

$$\mathcal{H} = J_1 \sum_{nn} S_i S_j + J_2 \sum'_{nnn} S_i S_j + J_3 \sum''_{nnn} S_i S_j - H \sum S_i. \tag{1}$$

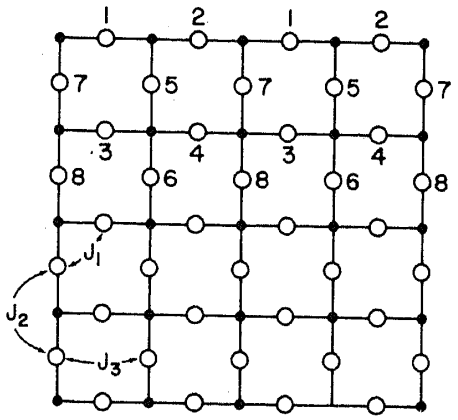

Figure 1. Cu–O basal plane showing the eight sublattices. Black dots stand for Cu atoms, and open circles stand for oxygen sites. Effective pair interaction J_1 couples the two oxygen sublattices; J_2 and J_3 operate on the sublattice.

The sum *nn* extends over all nearest neighbour interactions. The sums *nnn* extend over next nearest neighbour (*nnn*) bonds, where the prime indicates *nnn* bonds mediated by a Cu ion and the double primes without the Cu ion. The strength of the interaction parameters, confined to the range $[-1, 1]$, completely determines the energy of the oxygen-ion configurations and the stability of various ordered phases. Since the ortho I, ortho II and tetragonal phases are predicted by the present model, it is appropriate to define the sublattice magnetizations (see figure 1) and the order parameters corresponding to the different phases. We define the two order parameters for the ortho I and ortho II phases respectively as below:

$$M_{\mathrm{I}} = \left\{ \sum_{i=1}^{4} m_i - \sum_{i=5}^{8} m_i \right\} \Big/ 8, \tag{2}$$

$$M_{\mathrm{II}} = \{(m_1 + m_2) - (m_3 + m_4) + (m_5 + m_6) - (m_7 + m_8)\}/4, \tag{3}$$

where the eight sublattice magnetizations are defined by

$$m_\alpha = (8/N)\left\langle \sum_{i\in\alpha} S_i \right\rangle, \alpha = 1, 2, \ldots, 8. \tag{4}$$

It is clear that M_{I} is unity in the ortho I phase, zero in the tetragonal phase and takes on a value of 0·5 in the ortho II phase. Similarly M_{II} takes on a value of unity in the ortho II phase and goes to zero in the other two phases. The total magnetization is

$$M = (1/N)\sum_i \langle S_i \rangle. \tag{5}$$

The concentration x of oxygen can be represented in terms of the magnetization M as: $x = (1 + M)/2$.

In our Monte Carlo simulations, we considered a system of $N = 2 \times L \times L$ spins with periodic boundary conditions. L was measured in units of the lattice constant a. The simulations were performed using single spin-flip Glauber dynamics in the grand canonical ensemble, with the oxygen concentration varying as a function of temperature and magnetic field. Starting from an initial configuration, the system was

allowed to evolve according to the following algorithm: using pseudorandom numbers one generates a change of configuration $X \rightarrow X'$. This transition $X \rightarrow X'$ is taken to be the flip $S_i \rightarrow -S_i$ of a randomly chosen spin. The energy change $\delta U = \mathscr{H}(X') - \mathscr{H}(X)$ is then computed. The transition probability

$$W = \exp(-\delta U/k_B T)/[1 + \exp(-\delta U/k_B T)] \tag{6}$$

is then compared with a random number η, chosen uniformly in the range $[0, 1]$. If $W > \eta$ the transition is performed. If $W < \eta$ the attempted change X' is rejected and X is counted once more for averaging. The simulations were carried out for lattice sizes in the range: $24 \leqslant L \leqslant 96$. The data was obtained for typically ten to twenty thousand Monte Carlo steps per site. Figure 2 shows a typical example of 'raw data' of a Monte Carlo simulation.

Order parameter distribution functions were used to locate the phase boundary

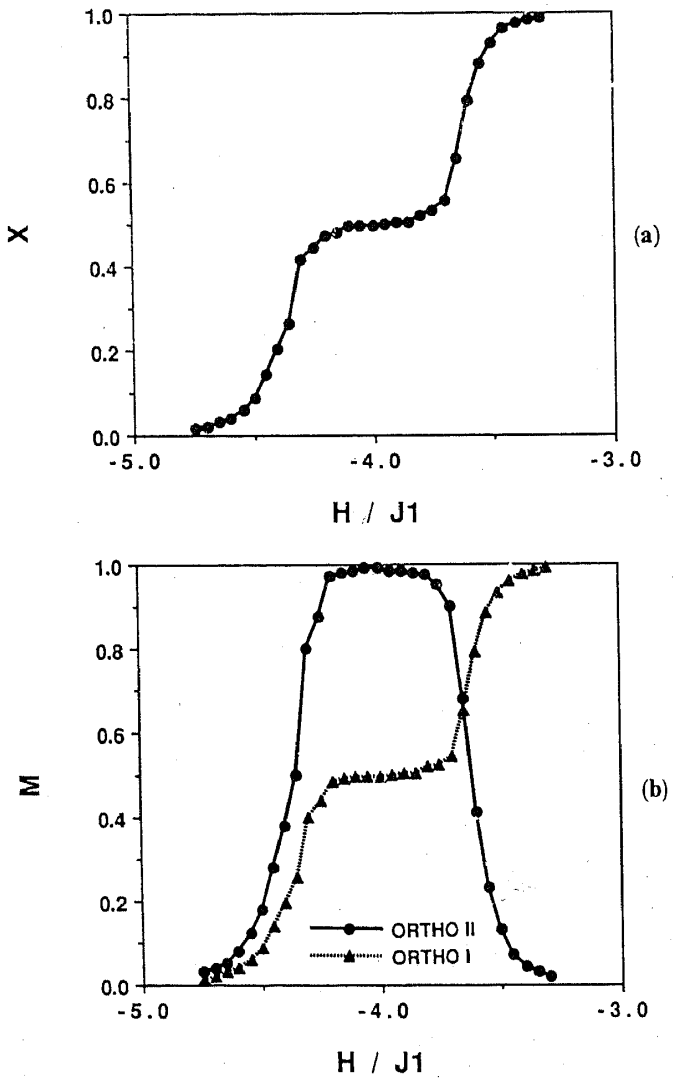

Figure 2. (**a**) Oxygen concentration x vs. magnetic field for $k_B T/J_1 = 0{\cdot}5$. (**b**) The order parameters for ortho I(O I) and 'double cell' ortho II(O II) phase vs. magnetic field for $k_B T/J_1 = 0{\cdot}5$.

and to determine the order of the transition (Mouritsen 1984). $P(\phi)d\phi$ is defined as the probability that the order parameter will take on a value in the range $[\phi, \phi + d\phi]$. The distribution functions P's for the concentration x, the ortho I and ortho II order parameters were used in this analysis. Away from the transition, $P(\phi)$ is a sharp, single peaked function. But in the transition region $P(\phi)$ becomes a broad/double peaked function indicating that more than one phase is being populated. At the transition temperature, the two peaks have the same intensity. For a second order transition, it is an important requirement that the two peaks move closer with increasing system size. An opposite size dependence in $P(\phi)$ indicates a first order phase transition. For a first order transition, the distribution function shows a bimodal form and the peak separation tends to increase and then saturate with the increasing lattice size. $P(\phi)$ is therefore indispensible for determining the nature of the transition.

3. Simulation results

The phase diagram obtained from the analysis of distribution function data from the Monte Carlo simulations is shown in figure 3. The dimensionless temperature scale $k_B T/J_1$ is the same as the one used by Wille and de Fontaine (1988), but is four times the scale used by Kikuchi and Choi (1989) and Aukrust *et al* (1990). This difference is due to a different choice of variables S_i's (or C_i's) in the basic Hamiltonian. We have also indicated the corresponding Kelvin scale along with a few experimentally observed phase transition points (OI to T). We now discuss the salient features of this new phase diagram.

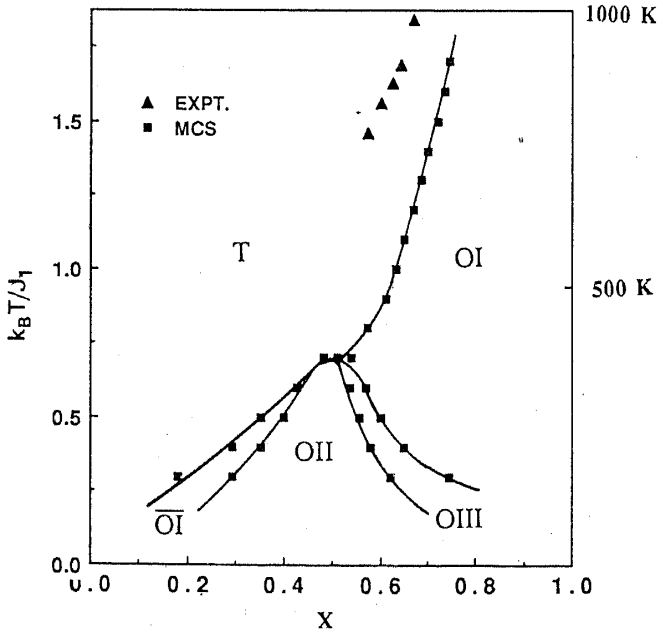

Figure 3. The phase diagram of $YBa_2Cu_3O_{6+x}$ as obtained from the analysis of distribution function data from Monte Carlo simulation. The interaction parameters are: $J_1 = 1{\cdot}0$, $J_2 = -0{\cdot}5$ and $J_3 = 0{\cdot}2$. Black triangles are the experimental data (Specht *et al* 1988).

3.1 *Low temperature, $x \geq 0{\cdot}5$ region*

This region is characterized by various orthorhombic phases. The superconducting O I phase dominates this region and extends from $x = 1{\cdot}0$ to $x = 0{\cdot}75$ $\sim 0{\cdot}55$ (depending on the temperature). Another dominant phase is the 'cell doubling' O II phase. Both these phases are predicted by the model and are observed in most of the published phase diagrams (Berera *et al* 1989; Zubkus *et al* 1989). A new feature however is the appearance of a new orthorhombic phase, labelled here as O III. Two distinct phase boundaries, both of second order, were observed between the O I and O II phases. Figure 4a shows the order parameter $P(x)$ as a function of x for three different magnetic field values. As the field value is changed, $P(x)$ changes from a single peak to a double peak indicating that two different states are being populated. As the field value is further increased, the double peak region goes over to a single

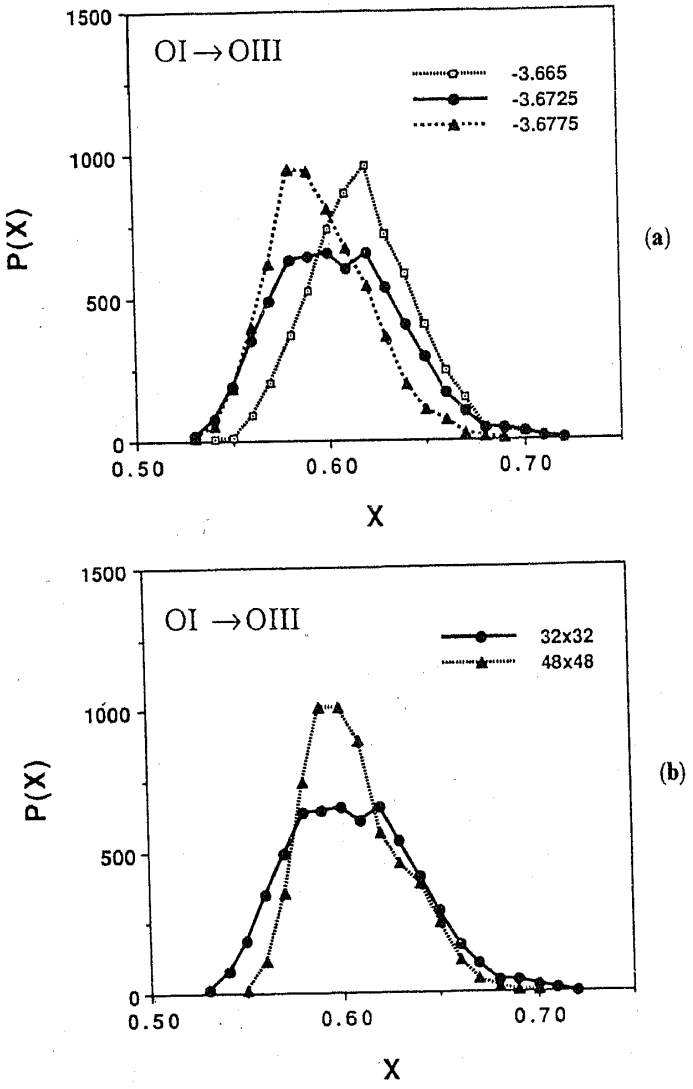

Figure 4. Plots of distribution function $P(x)$ vs. x for temperature $k_B T/|J_1| = 0{\cdot}5$ for O I to O III transition. (**a**). Plots of $P(x)$ for three different values of the field $H/|J_1|$. The magnitude of $H/|J_1|$ is indicated against the plot symbol. The lattice size for these simulations was 32×32. (**b**) Plots of $P(x)$ for two different lattice sizes at $H/|J_1| = -3{\cdot}6725$.

peak indicating that the system has undergone a transition from one state to another. For the sake of clarity, we have shown $P(x)$ values for only three magnetic fields. Simulation was carried out for a large number of points in the transition region. Similar results were obtained for $P(M_I)$ and $P(M_{II})$. Figure 4b shows a plot of $P(x)$ vs. x in the transition region for two different lattice sizes. As the lattice size increases, the two peaks come closer indicating the phase transition from O I to O III to be of second order. Figure 5 shows the $P(x)$ vs. x plots for O III to O II transition. Figure 4a shows the magnetic field dependence of $P(x)$, while figure 4b shows the effect of lattice size on peak separation. O III to O II transition is also of second order. For the purposes of comparison, in figure 6 we have plotted $P(M_{II})$ vs. M(ortho II) for different field values. While the double peak region is clearly visible, it is worth noting that M(ortho II) goes from 0·78 to 0·9 across the transition.

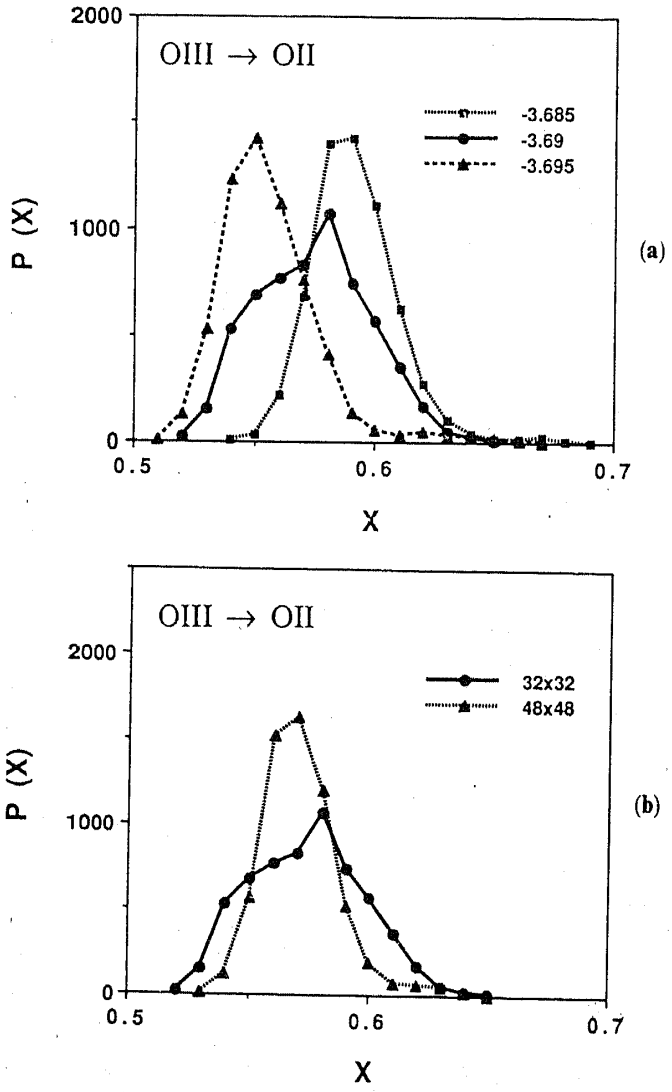

Figure 5. Plots of the distribution function $P(x)$ vs. x for temperature $k_BT/|J_1| = 0{\cdot}5$ for O III to O II transition. (**a**). Plots of $P(x)$ for three different values of the field $H/|J_1|$. The magnitude of $H/|J_1|$ is indicated against the plot symbol. The lattice size for these simulations was 32×32. (**b**). Plots of $P(x)$ for two different lattice sizes at $H/|J_1| = -3{\cdot}69$.

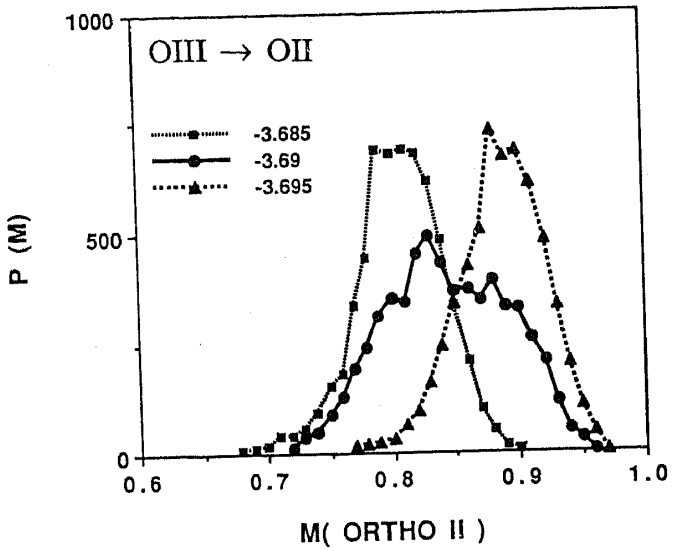

Figure 6. Plot of $P(M_{II})$ vs M(ortho II) for O III to O II transition at $k_B T/|J_1| = 0{\cdot}5$ for a 32×32 lattice. The magnitude of $H/|J_1|$ is indicated against the plot symbol.

3.2 *Low temperature, $x \leqslant 0{\cdot}5$ region*

The oxygen-deficient region of the phase diagram at low temperatures is also marked by two phase boundaries separating the tetragonal (T) and ortho II phase. The two boundaries come closer with increasing temperature, finally merging into a single phase boundary. The intermediate phase has been identified as the low density, low temperature orthorhombic phase O I that has been proposed by other authors (Kikuchi and Choi 1989; de Fontaine *et al* 1989, 1990). Figure 7a shows $P(x)$ vs. x plot across the O II and O I phase boundary for three different field values. A sharp peak in the O II region slowly decreases in intensity and a second peak starts developing at the cost of the first peak. As the field changes further, the first peak completely disappears leaving behind a sharp second peak. This also marks the end of the transition. In all these plots, the distribution function has not been normalized and the plots are typically for 10000 MCSS (Monte Carlo steps per site). Figure 7b shows the lattice size dependence of $P(x)$ across O II and O I phase transition. The narrowing of peaks with increasing size indicates this transition to be of second order. Figures 8a and 8b show the corresponding plots for O I to T transition region. In our earlier work (Khanna and Ananthakrishna 1992) using critical slowing down and relaxation time, τ, it is possible to miss out two such close lying transitions and to interpret them as a single transition. The distribution function approach using a number of order parameters offers a better resolution and two close lying transitions can be unambiguously identified.

3.3 *High temperature region*

The high temperature region is characterized by a single second order phase boundary across the O I and T phases. This result is consistent with most of the published phase diagrams. The main effect of lowering J_3 however was in restricting the range of various low temperature phases below $k_B T/J_1 = 0{\cdot}8$ (425 K). In most other works using a higher value of J_3, this range normally extended beyond $k_B T/J_1 \sim 1{\cdot}0$. We

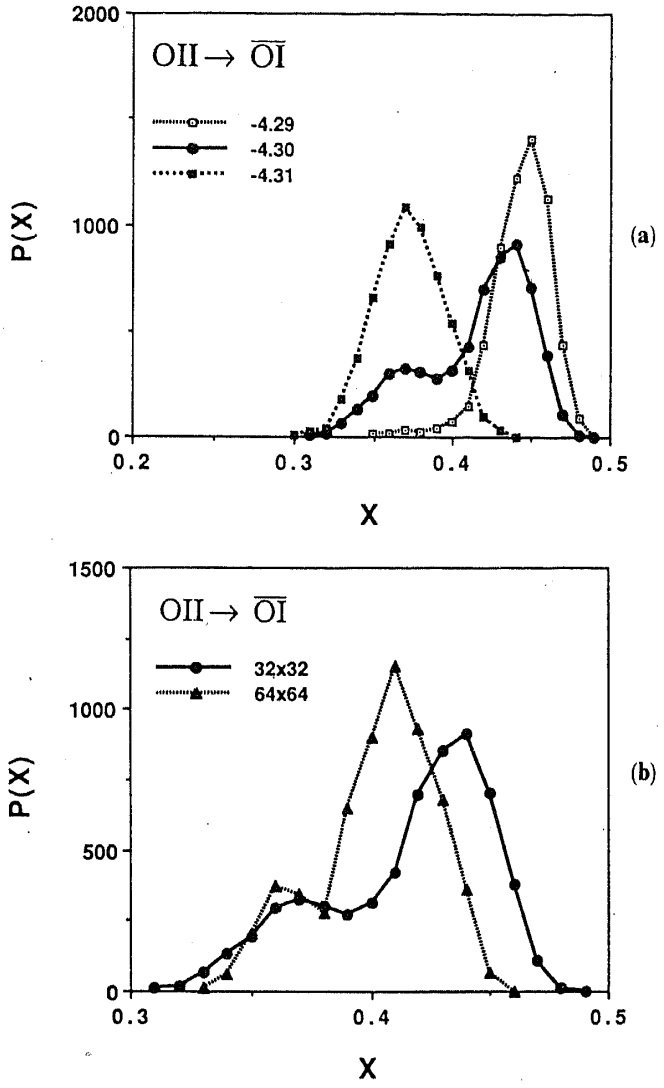

Figure 7. Plots of the distribution function $P(x)$ vs. x for temperature $k_BT/|J_1| = 0{\cdot}5$ for O II to $\overline{O}$ I transition. (**a**). Plots of $P(x)$ for three different values of the field $H/|J_1|$. The magnitude of $H/|J_1|$ is indicated against the plot symbol. The lattice size for these simulations was 32×32. (**b**). Plots of $P(x)$ for two different lattice sizes at $H/|J_1| = -4{\cdot}30$.

did not find any evidence of co-existing T and O I phases in this temperature regime. The phase boundary agrees well with the second-order T to O I transition points determined experimentally (Specht *et al* 1988) for different oxygen partial pressures.

4. Discussion and concluding remarks

Qualitatively the phase boundaries computed in this work are similar to those obtained by Wille and de Fontaine (1988), Kikuchi and Choi (1989), Aukrust *et al* (1990) and Zubkus *et al* (1991). There are three special features of our new phase diagram. First of all, the $\overline{O}$ I phase persists even for a very low value of J_3. In our earlier work for J_3 ranging between 0·3 and 0·5, we had found clear evidence for $\overline{O}$ I phase and for two second order phase boundaries separating O II and T phase. CVM calculations

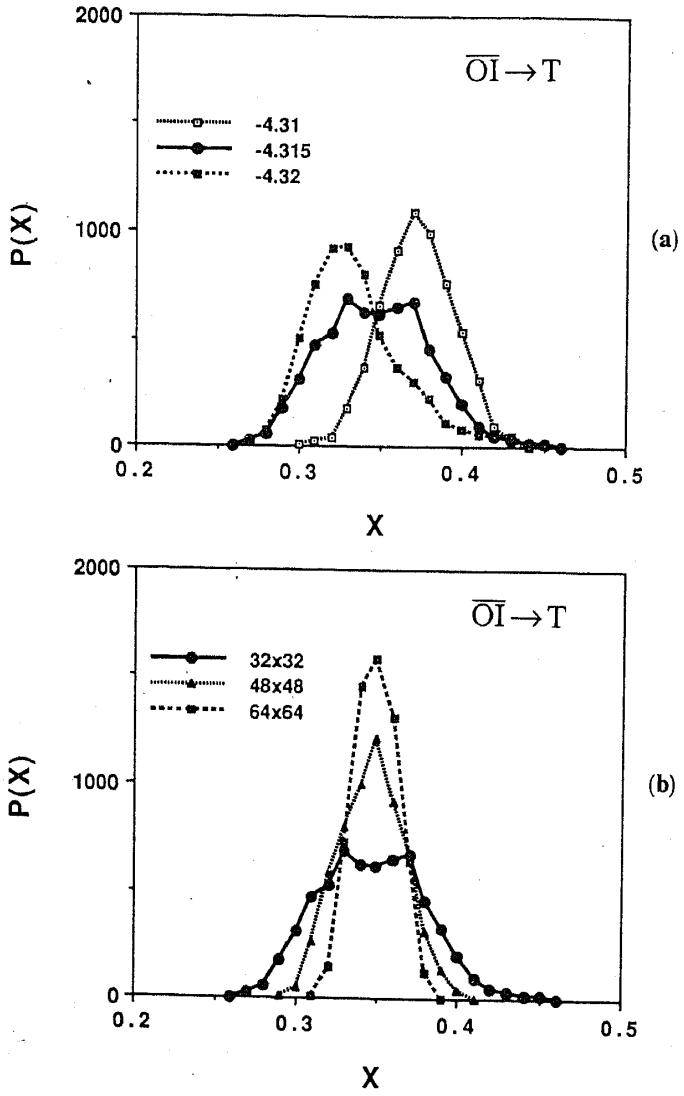

Figure 8. Plots of the distribution function $P(x)$ vs. x for temperature $k_B T/|J_1| = 0{\cdot}5$ for $\overline{OI}$ to T transition. (**a**). Plots of $P(x)$ for three different values of the field $H/|J_1|$. The magnitude of $H/|J_1|$ is indicated against the plot symbol. The lattice size for these simulations was 32×32. (**b**). Plots of $P(x)$ for two different lattice sizes at $H/|J_1| = -4{\cdot}315$.

of Kikuchi and Choi (1989) had also indicated the presence of a $\overline{O\,I}$ phase, but had predicted the transitions to be of first order. Recently Rikvold *et al* (1991) have looked at the macroscopic effects of local oxygen fluctuations in $YBa_2Cu_3O_{6+x}$. Using $J_3 = 0{\cdot}5$ and 32×32 lattice in their Monte Carlo simulation, they did not find evidence for $\overline{O\,I}$ phase and their lattice appeared to consist of short chains of oxygen atoms, randomly dispersed and oriented. This result is contrary to our results and that of many other authors (Kikuchi and Choi 1989; de Fontaine *et al* 1989, 1990; Bartlet *et al* 1989; Ceder *et al* 1990). In figure 9a, we show a typical lattice configuration plot in the $\overline{O\,I}$ phase. The tendency of oxygen is still to form long chains, though both the orientations were observed. These chains cannot be labelled as randomly dispersed and oriented. Our results agree well with those of Ceder *et al* (1990).

A second feature of our phase diagram is the appearance of a new orthorhombic phase, labelled here as O III, between O I and O II phases in $x > 0{\cdot}5$ region. A typical

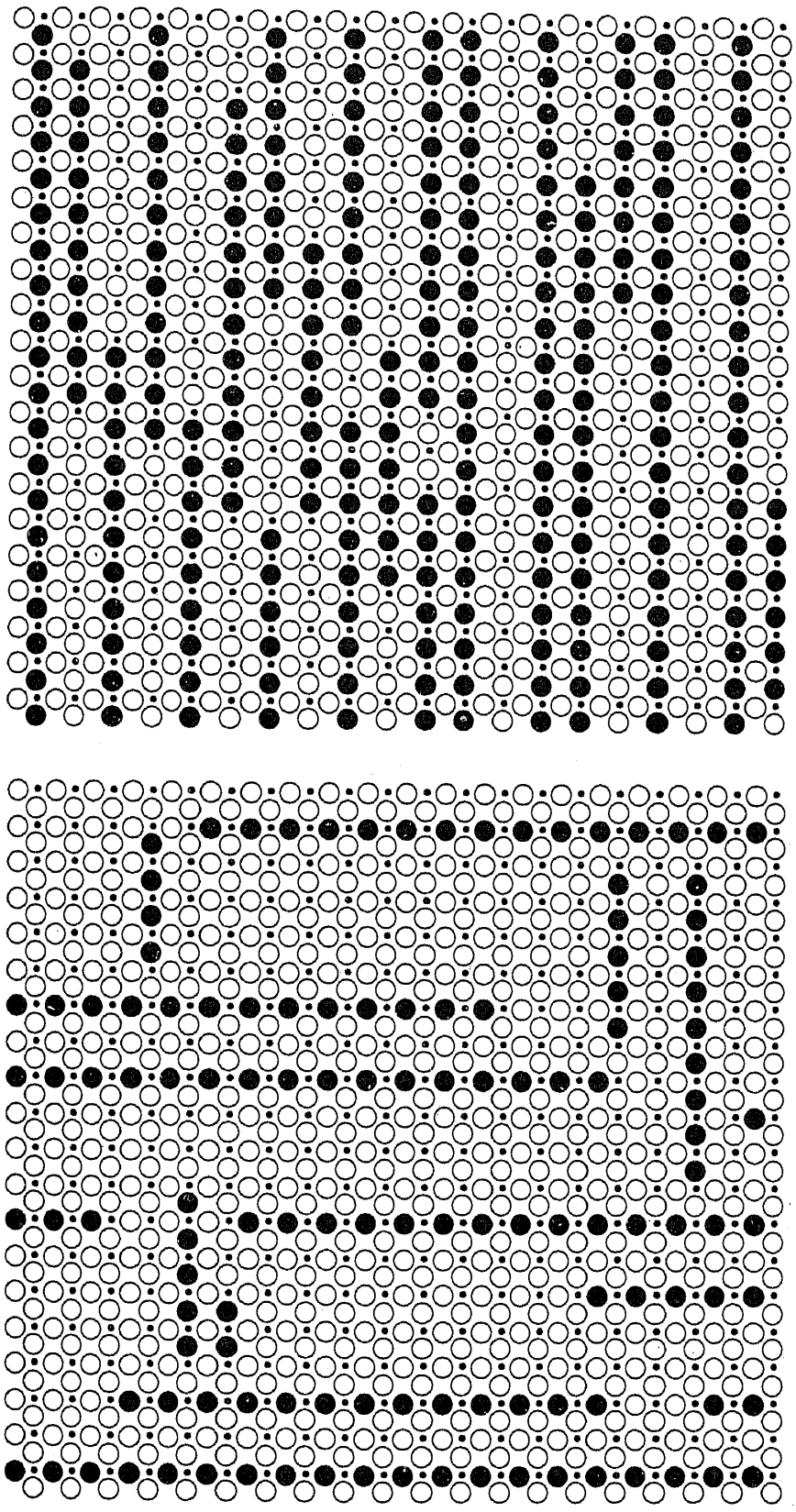

Figure 9. Lattice configuration plots obtained from Monte Carlo simulation. Small filled circles denote copper ions, large filled circles denote oxygen ions, and open circles denote vacant sites. **(a)** Lattice diagram in $O\bar{1}$ phase. Oxygen shows tendency to form long chains. **(b)** Lattice diagram in *O* III phase, ortho I, ortho II and 'Magneli phases' are present.

lattice configuration plot in the O III phase is shown in figure 9b. This phase is characterized by a high M(ortho II) parameter (typically $\sim 0{\cdot}75$) and appears to correspond to the formation of states of somewhat irregularly spaced parallel O–Cu–O chains with intermixed spacings of a to $5a$. These structures can be seen to correspond directly with the set of 'Magneli phases' described by Khachaturyan and Morris (1988). It is quite likely that a X-ray diffraction picture of this phase will contain diffuse spots corresponding to the positions for a Magneli phase. Experimentally also, Magneli phases have been observed as diffuse spots and not as sharp Bragg peaks (Werder *et al* 1988) implying that the Magneli phase does not span the complete lattice and only a small fraction of the system might have transformed into a Magneli phase. Our results with a small value of J_3 appear to be consistent with experimental observations.

The third significant feature of this phase diagram is the lowering of the temperature range of various low temperature phases and restricting them to below $k_B T/J_1 = 0{\cdot}8$ (425 K). For $J_3 = 0{\cdot}5$, this range had extended beyond 1·0. Sood *et al* (1988) and Radhakrishnan *et al* (1989) had observed the O I phase decomposing into co-existing T and O I phases after prolonged annealing at 473 K. This would indicate a first-order phase transition between T and O I phase. We found no evidence for such a decomposition. According to our phase diagram, the O I phase can transform directly to the T phase at 473 K, but co-existence of two phases is ruled out.

Zubkus *et al* (1991) have carried out a CVM calculation of the phase diagram using the same set of interaction parameters. Both phase diagrams appear to be quite similar and agree to the extent of predicting the presence of O I phase and lowering of the range of low temperature phases. CVM calculations using pair interactions from LMTO calculations ($J_1 = 6{\cdot}9$ mRy, $J_2 = -2{\cdot}4$ mRy ($J_2/J_1 = 0{\cdot}35$) and $J_3 = 1{\cdot}1$ mRy ($J_3/J_1 = 0{\cdot}16$)) have also observed similar features. Zubkus *et al* however do not see the presence of O III phase but observe a series of two phase regions ($T + O$ II, O I + O II, O I + O II) in the oxygen-deficient region of the phase diagram.

In view of these observations, we feel that lowering intra-sublattice repulsion to a small magnitude is a step in the right direction towards more realistic interaction parameters for $YBa_2Cu_3O_{6+x}$ as it is able to offer explanation for a large number of experimental observations. It is expected that this present excercise will help in establishing the correct phase diagram of $YBa_2Cu_3O_{6+x}$ and may help in clarifying the relation between oxygen content and T_c in this compound.

References

Aukrust T, Novotny M A, Rikvold P A and Landau D P 1990 *Phys. Rev.* **B41** 8772

Bartlet N C, Einstein T L and Wille L T 1989 *Phys. Rev.* **B40** 10759

Beech F, Miragalia S, Santoro A and Roth R S 1987 *Phys. Rev.* **B35** 3608

Berera A, Wille L T and de Fontaine D 1989 *J. Stat. Phys.* **50** 1245

Beyers R, Ahn B T, Gorman G, Lee V Y, Parkin S S P, Ramirez M L, Roche K P, Vanquez J E, Gur T J and Huggins R A 1989 *Nature (London)* **340** 619

Beyers R and Shaw T 1989 *Solid state physics* (eds) H Ehrenrich and D Turnbull (New York: Academic) Vol. 42 p. 135

Cava R J, Batlogg B, Chen C H, Rietman E A, Zahurak S M and Weber D 1987 *Phys. Rev.* **B36** 5719

Ceder G, Asta M, Carter W C, Kraitchman M, de Fontaine D, Mann M E and Sluiter M 1990 *Phys. Rev.* **B41** 8698

Chen C H, Werder D J, Schneemeyer L F, Gallagher P K and Waszczak J V 1988 *Phys. Rev.* **B38** 2888

de Fontaine D, Wille L T and Moss S C 1987 *Phys. Rev.* **B36** 5709
de Fontaine D, Mann M E and Ceder G 1989 *Phys. Rev. Lett.* **63** 1300
de Fontaine D, Ceder G and Asta M 1990 *Nature (London)* **343** 544
Jorgenson J D, Beno M A, Hinks D G, Soderholm L, Volin K J, Hitterman R J, Grace J D, Schuller I K, Segre C V, Zhang K and Kleefisch M S 1987 *Phys. Rev.* **B36** 3608
Khachaturyan A G and Morris Jr. J W 1987 *Phys. Rev. Lett.* **59** 2776
Khachaturyan A G and Morris Jr. J W 1988 *Phys. Rev. Lett.* **61** 215
Kikuchi R and Choi J S 1989 *Physica* **C160** 347
Khanna R and Ananthakrishna G 1992 *Physica* **C195** 59
Khanna R, Welberry T R and Ananthakrishna G 1992 *Physica* **C197** 57
Mamsurova L G, Pigalskiy K S, Sakun V P, Shushin A I and Scherbakova L G 1990 *Physica* **C167** 11
Mouritsen O G 1984 *Computer studies of phase transitions and critical phenomenon* (New York: Springer Verlag) p. 18.
Radhakrishnan T S, Janaki J, Rao G V N, Kalavathi S, Sastry V S, Hariharan Y, Janwadkar M P, Govindarajan K, Parameswaran P and Sridharan O M 1989 *Pramana – J. Phys.* **32** L705
Rayes-Gasga J, Krekel T, van Tendaloo G, van Landyut J, Amlinckx S, Bruggink W H M and Verwij M 1989 *Physica* **C159** 831
Rikvold P A, Novotny M A and Aukrust T 1991 *Phys. Rev.* **B43** 202
Sood A K, Sankaran K, Sankara Sastry V, Janwadkar M P, Sundar C S, Janaki J, Vijyalakshmi S and Hariharan Y 1988 *Physica* **C156** 720
Specht E D, Sparks C J, Dhere A G, Brynestad J, Cavin O B, Kroeger D M and Oye H A 1988 *Phys. Rev.* **B37** 7426
Stolze J 1990 *Phys. Rev. Lett.* **64** 970
van Tendaloo G, Zandbergen H W and Amelincks 1987 *Solid State Commun.* **63** 603
Werder D J, Chen C H, Cava R J and Batlogg B 1988 *Phys. Rev.* **B38** 5130
Wille L T and de Fontaine D 1988 *Phys. Rev.* **B37** 2227
Zanbergen H W, van Tendaloo G, Okabe T and Amlinckx S 1987 *Phys. Stat. Solidi* **A103** 45
Zubkus V E, Lapinskas S and Tornau E E 1989 *Physica* **C159** 501
Zubkus V E, Tornau E E, Lapinskas S and Kundrotas P J 1991 *Phys. Rev.* **B43** 13112